

UDC 622.24

M. H. KADKHODAEI<sup>1</sup>, Ph.D. student  
 R. BAGHERPOUR<sup>1</sup>, Professor, bagherpour@iut.ac.ir  
 A. NADRI<sup>2</sup>, MSc of Mining Engineering

<sup>1</sup>Isfahan University of Technology, Department of Mining Engineering, Isfahan, Iran

<sup>2</sup>Anarak Mine Manager, Isfahan, Iran

## EXPERIMENTAL INVESTIGATION AND OPTIMIZATION OF THE PENETRATION RATE OF LARGE-SCALE DTH DRILLING IN COPPER MINES

### Introduction

In today's world, with the development of mining, oil, and construction projects, rock excavation becomes more and more important. Although various methods using different equipment have been proposed for rock breaking until today, the mechanical excavation method has always been the most cost-effective and most suitable method and is currently widely employed in the fields of mining and civil engineering. One of the most widely used methods of rock excavation is rock drilling, which is commonly utilized to create blast holes, coring, exploration of minerals, extraction of oil and gas sources, installation of support system (for example, rock bolts), and so on [1, 2].

The efficiency of drilling is also linked to the extra costs incurred by using a platform, which may amount to tens of thousands of dollars each day [3]. One of the most critical parameters for planning drilling operations and estimating costs is the rate of penetration (ROP). The ROP depends on various variables, including operational parameters, as well as geological conditions and rock properties [4, 5]. Consequently, optimizing the ROP in drilling as the first step in mine to mill optimization leads to cost reduction and enhanced production. Therefore, according to the importance of the subject, various studies have been conducted in order to evaluate the ROP based on rock properties [6–18] and operational parameters [19–26].

In the literatures, specifically in works by Bourgoyne and Young [27] and Hegde et al. [28], several ROP equations have been developed as functions of various parameters, including bit properties, formation strength, mud properties, bit diameter, bit design, Rotations Per Minute, Weight on Bit, and bit hydraulics. These equations are generated from the study of theory and experiments. The ROP for percussion drilling has been proposed by Hustrulid and Fairhurst [29] based upon theoretical and experimental studies according to Eq. (1).

$$ROP = \frac{E_j \cdot f \cdot T_r}{A \cdot SE}, \quad (1)$$

where  $A$  is drill hole area ( $m^2$ );  $SE$  is specific energy ( $Nm/m^3$ );  $T_r$  is energy transfer rate;  $f$  is blow frequency (blow/min);  $E_j$  is energy per blow (Nm).

Kahraman [30] has used the twin-logarithmic model, as one of the non-linear methods, to develop a DTH drilling ROP model (Eq. (2)).

$$ROP = 3.24 \frac{(Pd)^{0.826}}{R_n^{1.9}}, \quad (2)$$

where  $P$  is operating pressure (bar);  $R_n$  is Schmidt hammer rebound number (N-type);  $d$  is piston diameter (mm).

*Optimizing the conditions of the drilling operation to achieve the maximum penetration rate (ROP) is essential as the initial step in mine-to-mill optimization. This study mainly focuses on optimizing the operational-scale drilling operation conditions of the drill wagon. For this purpose, two operational parameters (feed rate pressure and air flushing pressure) were identified as influential factors affecting the ROP. Various operational conditions were subsequently established using the Taguchi algorithm. Based on these conditions, drilling operations were conducted at the Anarak copper mine in Isfahan, Iran. Finally, the optimal operating conditions for different mine zones were developed. The results of the optimization showed that with the increase of copper grade and the decrease of rock strength, air flushing pressure has the most significant impact on the drilling ROP. Subsequently, a model was developed using three intelligent methods: Artificial Neural Network (ANN), Random Forest (RF), and Support Vector Machine (SVM). These models aimed to predict the ROP within the Python environment, utilizing a database comprising 170 drilling operations conducted at the Sarcheshmeh copper mine in Kerman, Iran. This database includes parameters that affect drilling ROP, including feed rate pressure, air flushing pressure, and geological strength index. To evaluate the performance of the developed models, three performance evaluation criteria (such as variance account for, normalized root mean square error, and coefficient of determination) were used based on the training database. The results showed that the RF model has a higher performance than the SVM and ANN model. Furthermore, the RF model was utilized for predicting the ROP in drilling operations at the Anarak copper mine. After conducting drilling operations in this mine and comparing the results, it was found that the RF model predicts the ROP with an accuracy of 83.8%. Therefore, the RF model can be confidently utilized in drilling projects with low uncertainty.*

**Keywords:** drilling, penetration rate, taguchi, optimization, machine learning

**DOI:** 10.17580/em.2024.02.14

Considering the importance of the issue and the immediate impact of ROP on drilling costs and production planning, it is imperative to assess the ROP in relation to operational conditions and rock properties. In addition, optimizing drilling conditions to increase ROP as the initial step of mine-to-mill optimization increases its importance.

After a comprehensive analysis of previous research conducted by other researchers, it has been determined that all of these studies only evaluate the effect of operational parameters and rock properties individually on the ROP, and the study and optimization of drilling operation conditions on a large scale has not been done. In this study, the prediction and optimization of the ROP for DTH drilling in copper mine operations, using the rotary percussion drilling method, are discussed. For this purpose, first by using smart methods on a database, according to the operational parameters and rock properties that affect the ROP, models are developed to predict the ROP. Subsequently, using the Taguchi optimization algorithm on the drilling operation of the Anarak copper mine drill wagon, the optimal operating conditions are determined with the aim of maximizing the ROP. **Figure 1** shows the flow chart of this study.

### Drilling optimization

Anarak copper mine is a sulfide copper mine located in the north-east of Isfahan province (Central Iran). The Anarak plutonic complex includes a wide range of rock types, from Gabbro-Monzogabbro to Alkali granite, spanning from the Upper Precambrian to the Quaternary

period. There are five main sulfide minerals in this deposit: Chalcocite, Chalcopyrite, Covellite, Molybdenite, and Bornite. In this mine, the drilling of blast holes is carried out using the ROC-D65 drill wagon (Fig. 2).

The Taguchi optimization method has been used to determine the optimal operational conditions for drilling in the Anarak Mine. The Taguchi Technique is a robust design methodology within the field of design of experiments. It is primarily used for improving the quality and performance of products and processes while minimizing variation and the occurrence of defects [31]. This technique generates a unique design of orthogonal arrays that can effectively explore the entire parameter space with just a minimal number of experiments. Subsequently, the analysis of the test results employs a statistical metric known as the signal-to-noise ratio (S/N). This ratio provides insights into both the average and the variation of the experimental results within this method and is determined according to Eq. (3) for maximization problems [32].

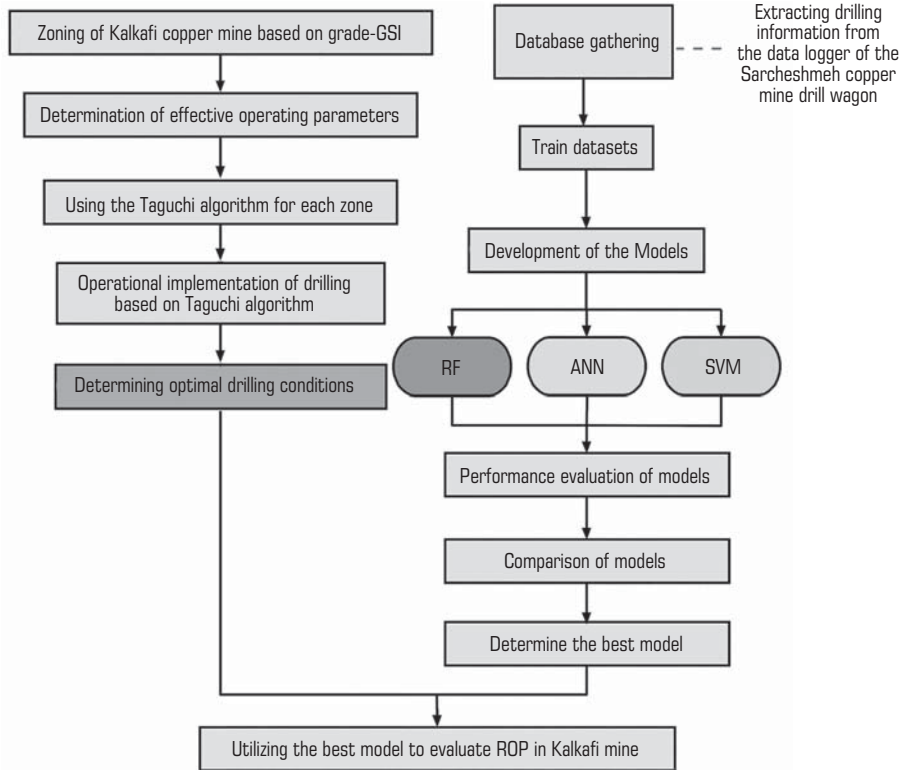


Fig. 1. The flow chart of this study



Fig. 2. The ROC-D65 drill wagon of Anarak mine

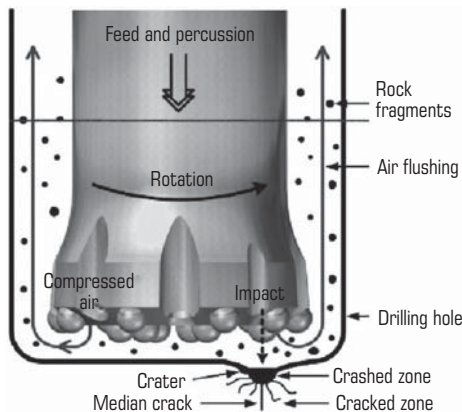


Fig. 3. The schematic view of drilling process [39]

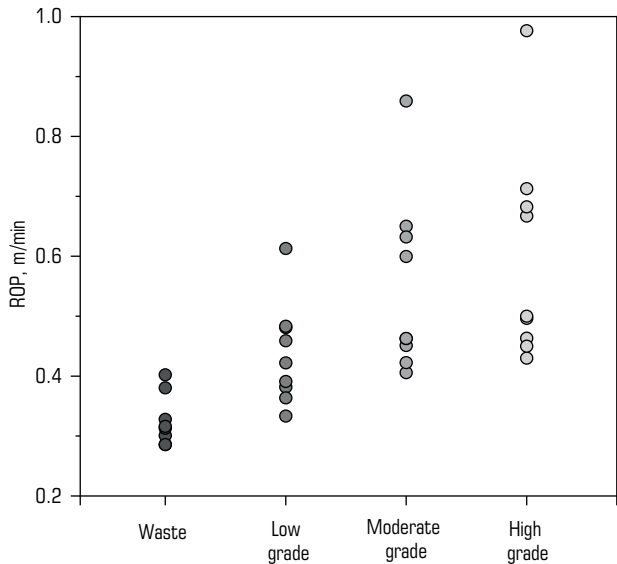
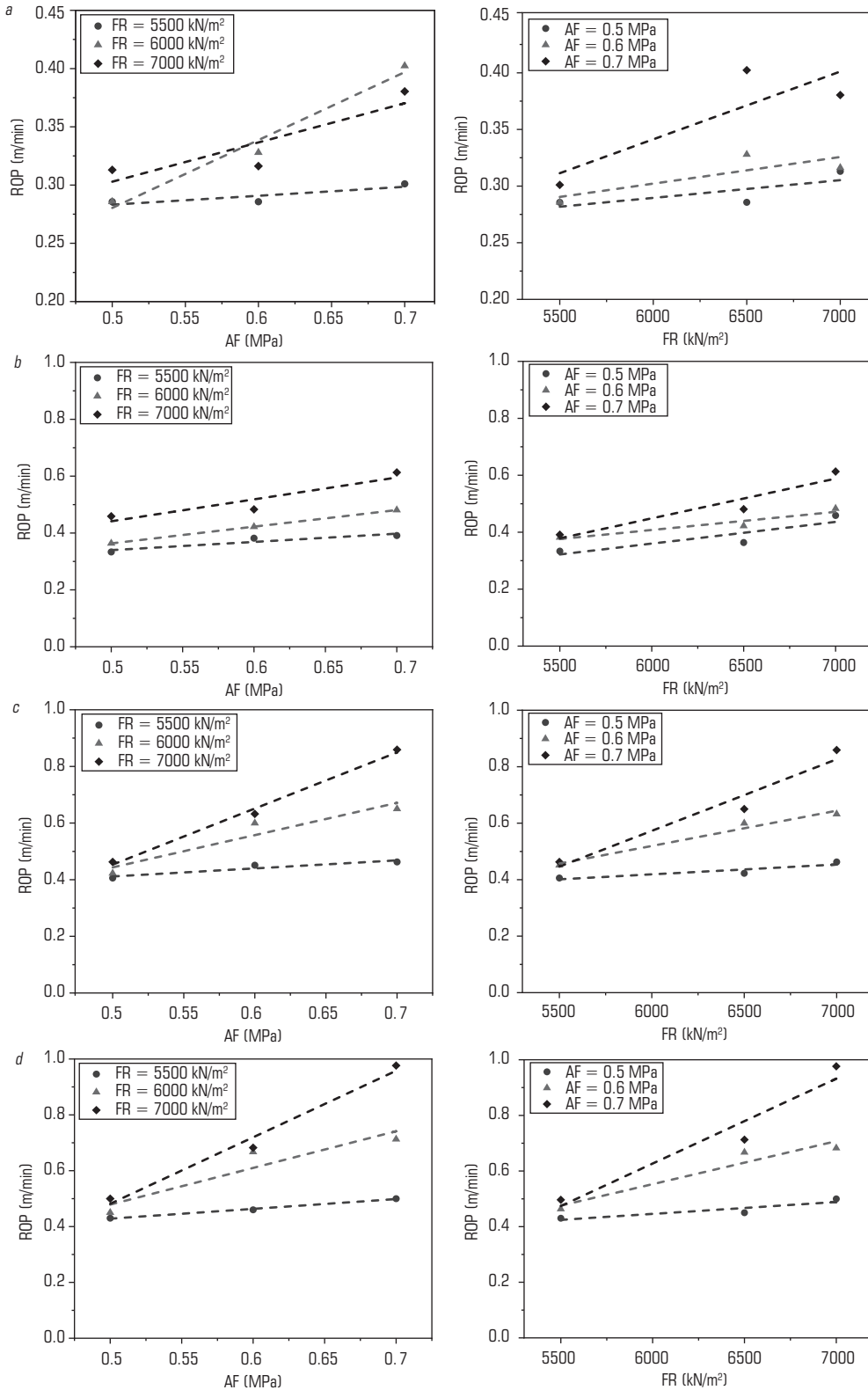


Fig. 4. The distribution of ROP in each zone

Table 1. Classification of grade-GSI of Anarak mine

Level	Grade	GSI	Representative color	Code
High grade	>0.45	<40		1
Moderate grade	0.3–0.45	40–50		2
Low grade	0.15–0.3	50–60		3
Waste	<0.15	>60		4



**Fig. 5. The relationship between FR and AF with the ROP:**  
 a – Waste; b – Low grade; c – Moderate grade; d – High grade

$$S/N \text{ ratio}(\eta) = -10 \log_{10} \frac{1}{n} \sum_{i=1}^n \frac{1}{y_i^2}, \quad (3)$$

where  $y_i$  is the response value for an experimental condition.

Due to its simplicity and high performance, this method has been widely used in experimental design and optimization in engineering studies [33–38].

In the process of choosing the operating parameters for the drill wagon based on rotary percussion drilling method, the focus has been on selecting those parameters that exert the most significant influence on the ROP. To achieve this objective, two key parameters, namely the feed rate pressure (FR) and air flushing pressure (AF), have been selected. These parameters exhibit the most impact on the ROP while simultaneously having the least effect on the machine stress. In other words, according to Fig. 3, these two parameters possess the most significant influence on the interaction between the rock and the drilling bit. Unlike the rotation speed, adjustments to these parameters result in minimal stress on the drilling machine.

To determine the optimal conditions of drilling operations with the aim of maximizing ROP, two operational parameters FR and AF were entered into the Taguchi algorithm in the operating range of 5500 to 7000 kN/m<sup>2</sup> and 0.5 to 0.7 MPa, respectively, and based on the proposed drilling plan, operations were carried out in Anarak mine. It should be noted that throughout all the tests, the rotation speed remained constant at 55 RPM, and the diameter of the hole was 110 mm (with air flushing holes having a diameter of 17 mm). It should be noted that during the execution of the tests, drill bits with the same geometry were used. In addition, the compressor of this drill wagon is an Atlas Copco XRX 10 (two-stage screw type compressor) and is capable of producing air pressure up to 3 MPa. Additional specifications of this machine can be found in the relevant catalogs and studies conducted in this field using this machine [40]. It should be noted that the range of AF changes has been selected according to the type of rock being drilled and its impact on drilling performance in such a way that with an excessive increase in AF, the penetration rate variations remain constant and do no effect on drilling performance. According to the grade data available, this mine encompasses four distinct grade zones (waste, low grade, moderate grade, and high grade). For every drilled hole, the geological strength index (GSI) was evaluated and subsequently

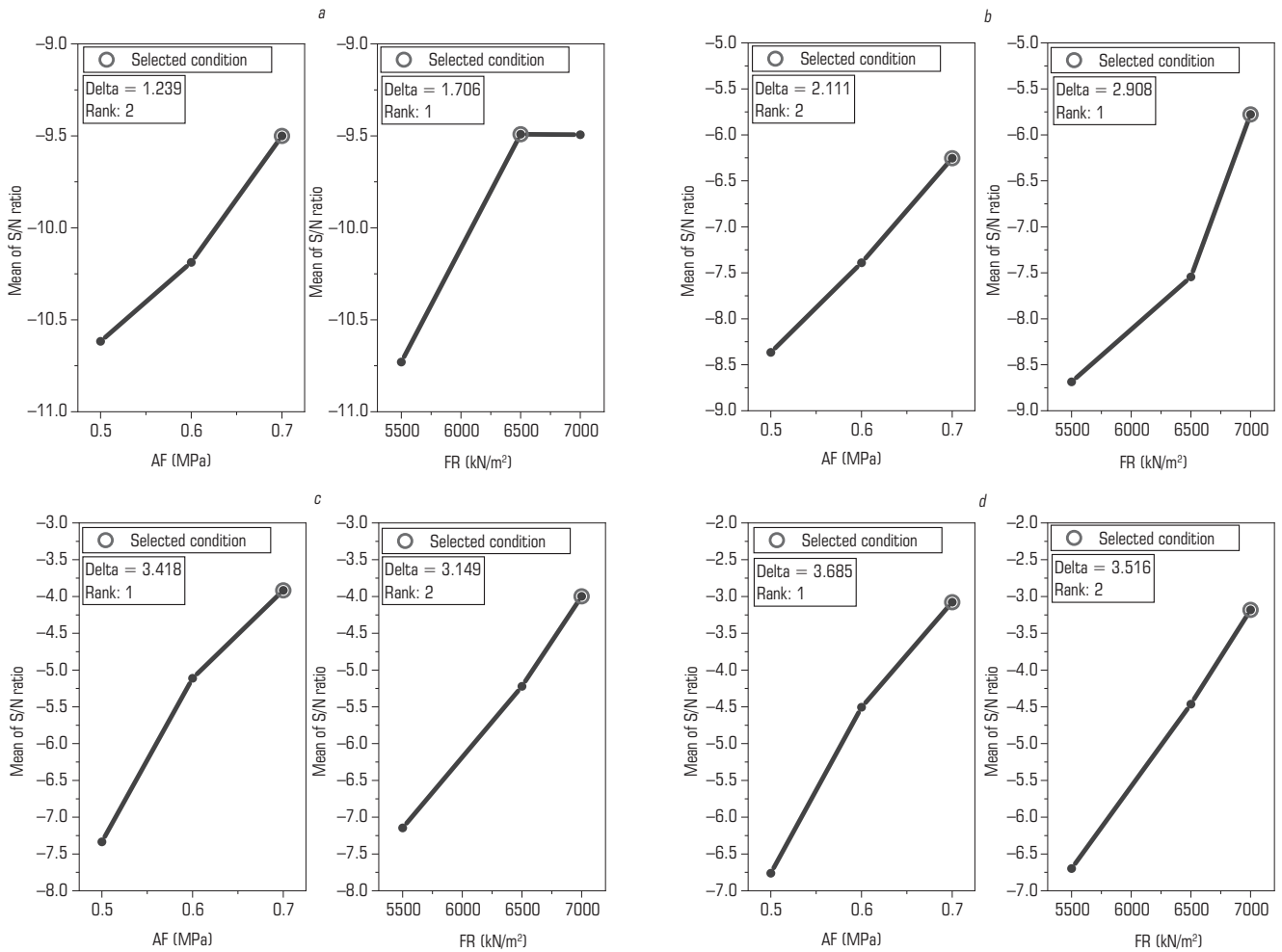


**Fig. 6. The S/N plot of the grade zones based on the Taguchi algorithm:**  
*a* – Waste; *b* – Low grade; *c* – Moderate grade; *d* – High grade

categorized into four classes according to **Table 1**. The GSI represents the properties of the rock mass being drilled, encompassing the strength characteristics, surface condition of the discontinuities, and deformation characteristics of the rock mass [41]. In drilling activities, in cases where there is no available information about the conditions of the rock mass, it is possible to estimate the GSI by assessing the surface conditions and the structure of the rock mass [42] deformation modulus, strength properties, and Poisson's ratio for an appropriate design of tunnels, caverns, and other engineering structures. The distinctiveness of this system over the rock mass rating (RMR).

According to the developed Taguchi plan, the drilling operation was done for each zone separately and in order to reduce the operation error, each test was repeated 9 times (totally 334 holes) and the average ROP was considered as the result of each operational condition. **Figure 4** shows the distribution of ROP in each zone. **Figure 5** shows the relationship between FR and AF with the ROP for each zone. According to the figure, there is a direct correlation between AF and ROP. This relationship is primarily attributed to the fact that when AF increases, fragments are quickly removed from the hole, allowing the drill bit to make contact with a clean rock surface. This leads to heightened rock crushing and ultimately results in an increase in ROP. Conversely, when the amount of AF is low, fragments remain within the hole, causing the drilling bit to impact these fragments. This situation leads to heightened energy consumption, increased tool wear, and reduction in ROP. Furthermore, as FR increases, ROP also shows an increase. However, if it surpasses a specific threshold,

ROP begins to decrease (Fig. 5, *a*). In other words, an excessively high increase in the FR results in a reduction in the ROP. Eventually, the drill bit becomes stuck, causing damage to the couplings, rods, and ultimately the drilling machine. **Figure 6** shows the S/N plot of the grade zones based on the Taguchi algorithm. According to the figure, when the grade of copper ore increases and its resistance decreases, AF becomes the effective parameter in the drilling operation (Fig. 6, *c* and *d*). Conversely, when the rock resistance increases, FR becomes a significant parameter in the drilling operation (Fig. 6, *a* and *b*). This occurs because the lower resistance of the rock results in a greater volume of drilling fragments, necessitating higher air pressure for their removal from the hole. Consequently, in such instances, the operational parameter AF assumes a more pivotal role in increasing the ROP.

#### Database description

In order to evaluate the ROP of drill wagons, a database of drilling wagons has been collected at the Sarcheshmeh copper mine, Iran. Sarcheshmeh copper mine is located in the southwest of Kerman province (southeast of Iran) at an elevation of 2600 m above sea level (56° 51' 54" E and 29° 57' 31" N). The main minerals found in this mine are categorized into two groups: sulfide minerals (Chalcocite, Chalcopyrite, Covellite, Bornite, and Molybdenite) and oxide minerals (Cuprite, Malachite, Tenorite, and Azurite). The collected database includes the drilling information of 170 blast holes using a drill wagon, which is obtained directly from the drilling log. This database includes AF, FR, and GSI as input parameters and ROP as output

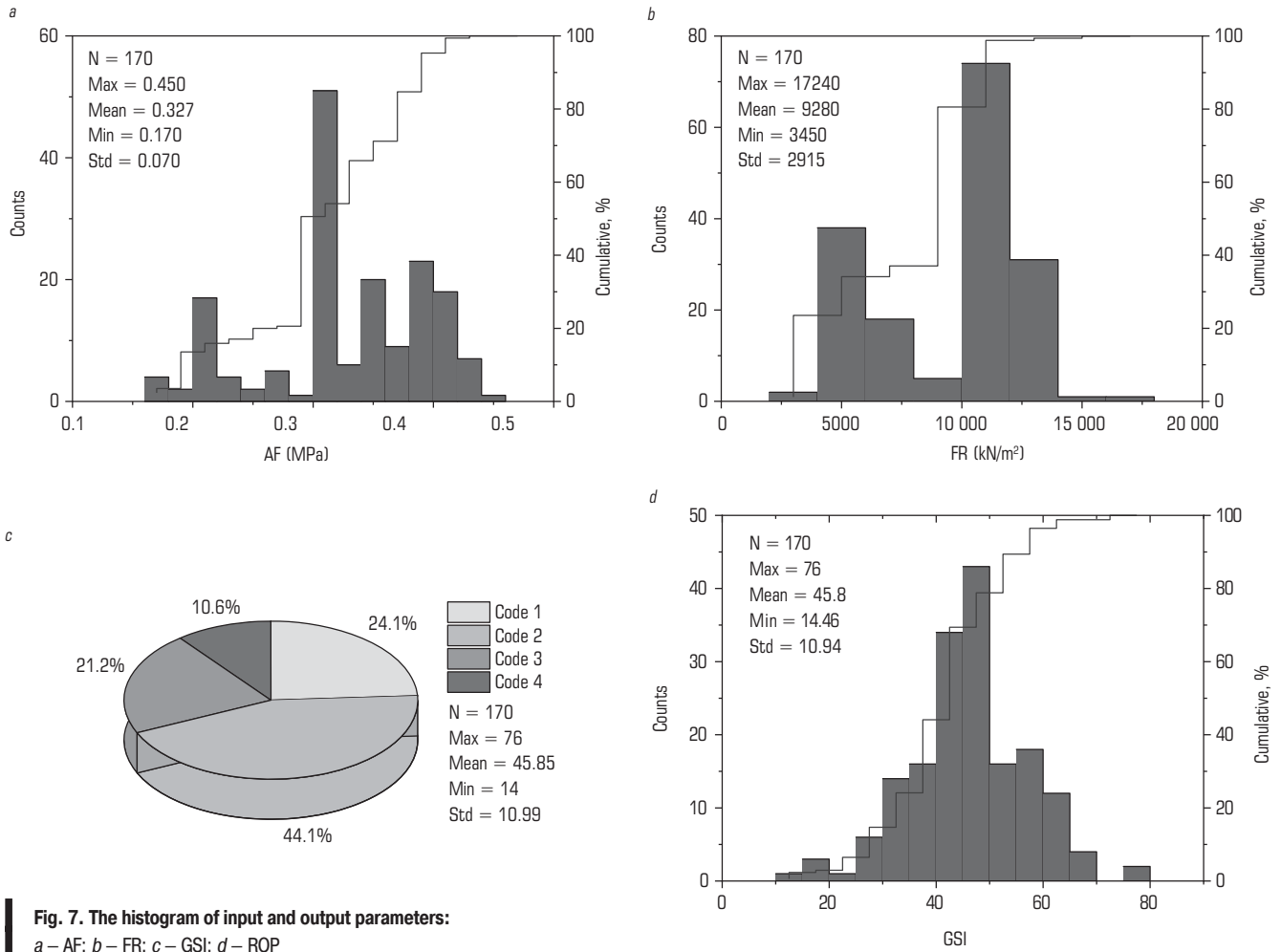


**Fig. 7. The histogram of input and output parameters:**  
 a – AF; b – FR; c – GSI; d – ROP

parameter. **Figure 7** shows the histogram of input and output parameters. It should be noted that similar to the grade-GSI classification of Anarak copper mine (see Table 1), the GSI parameter of Sarcheshme copper mine was also classified into four classes (code 1, 2, 3 and 4 according to Fig. 7, c). **Figure 8** shows the relationship between database parameters. According to the figure, the AF and FR parameters have a direct relationship with ROP, while the GSI parameter exhibits an indirect relationship with ROP, which is in line with the drilling mechanism.

**Model Development**  
**Support vector regression**

The support vector machine (SVM) is an efficient learning system that leverages the inductive principle of minimizing structural errors, ultimately resulting in a general optimal solution. The SVM algorithm is one of the machine learning algorithms and it is also classified as a supervised training method that establishes a relationship between the input data and the value of the

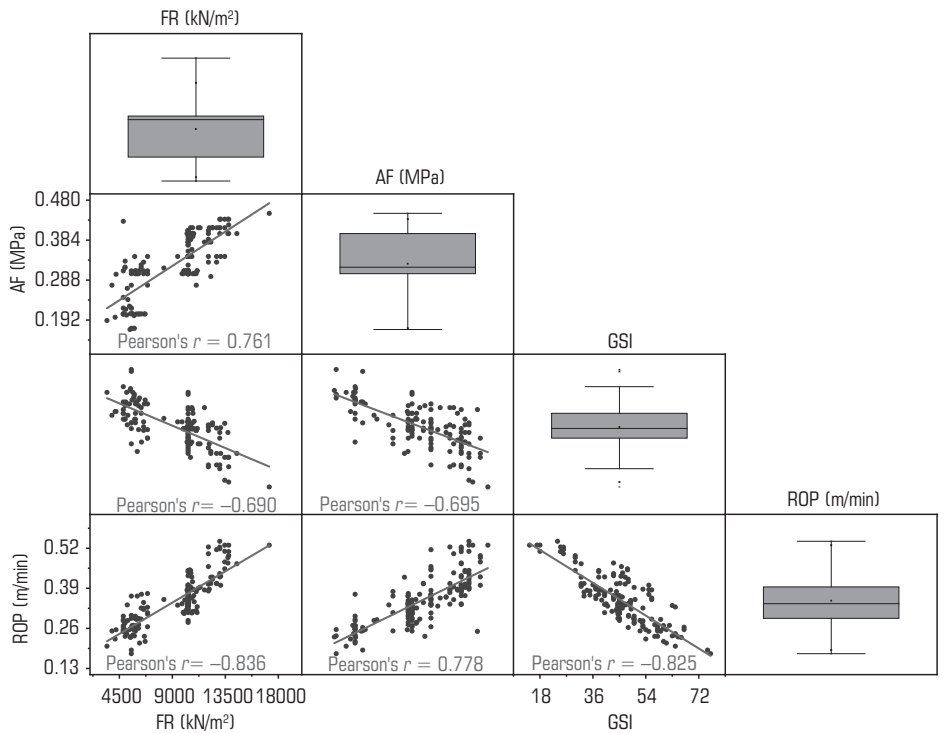


**Fig. 8. The relationship between database parameters**

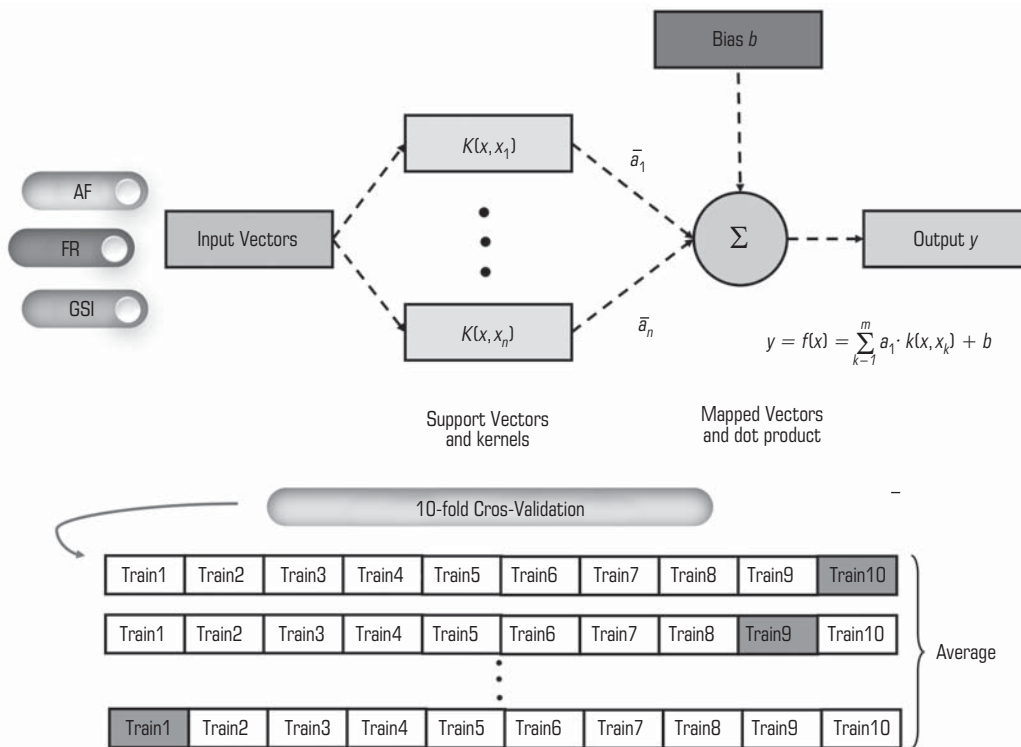


Fig. 9. The schematic representation of the implemented SVR algorithm

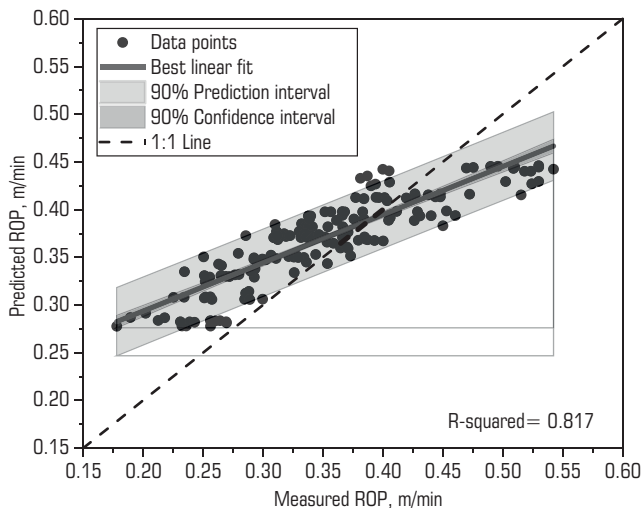


Fig. 10. The relationship between predicted and measured values of SVR model

dependent variable based on structural risk minimization [43]. In contrast to neural network algorithms, which attempt to characterize the intricacies of functions within the input space, this algorithm transforms non-linear data into a higher-dimensional space and employs non-linear functions within this new space. Generally, the algorithm’s performance in regression problems involves the mapping of input vectors into a multidimensional space. Subsequently, a hyperplane is generated to separate the input vectors with the maximum possible distance [44]. In order to develop the predictive ROP model using the Support Vector Regression (SVR) algorithm, it has been coded within the Python 3.11 environment and executed on the database. In this algorithm, radial basis function (RBF) kernel is employed in conjunction

with a 10-fold cross-validation approach. Figure 9 shows the schematic representation of the implemented SVR algorithm. Figure 10 shows the relationship between predicted and measured values of SVR model.

**Random forest**

The Random Forest (RF) method is founded on novel techniques for aggregating information, wherein a substantial number of decision trees are generated, and subsequently, all these trees are combined to make predictions [45]. The RF algorithm relies on an ensemble of decision trees and is currently considered one of the top-performing learning models. Generally, the RF predictive model is built by averaging the outcomes of numerous pertinent decision trees, often yielding highly accurate predictions for a wide range of datasets. The RF is constructed

using a set of trees considering ‘n’ independent data [46, 47]. Due to the Law of Large Numbers (LLN), the algorithm does not tend to overfit, making it a highly effective method for prediction [48]. Figure 11 shows the training procedure of the RF algorithm [49]. In order to develop the predictive ROP model using the RF algorithm, it has been coded within the Python 3.11 environment and executed on the database. It should be noted that the node size variable, signifying the number of leaves in each branch, was determined through trial and error. Figure 12 shows the relationship between predicted and measured values of RF model.

**Artificial neural network**

An Artificial Neural Network (ANN) emulates the intricate and parallel computational system of the brain, consisting of numerous simple processing units known as neurons. A neuron acts as a simplified representation of a biological neuron. The number of neurons used can vary depending on the specific problem being addressed [50]. The ANN comprises at least three layers: an input layer, a hidden layer, and an output layer, with each layer housing numerous interconnected neurons. These interconnections are formed through weighted connections. Essentially, a neural network functions as an intelligent system capable of predicting output patterns by recognizing specific input patterns [51]. In order to create an ANN model, different methods are used for connecting neurons. Many researchers have reported that feedforward-back-propagation (FF-BP) is the most widely utilized type of ANN in various fields of science and engineering [52–54] flyrock and back-break. Therefore, proper predicting and subsequently optimizing these impacts may reduce damage on facilities and equipment. In this study, an artificial neural network (ANN). One of the most well-known FF-ANNs is the multi-layer perceptron (MLP) neural network, which consists of several neurons or nodes in three layers that are connected to each other by weights and can solve complex engineering problems [55]. Figure 13 shows the schematic representation of the implemented MLP algorithm [56]. In order to develop the predictive ROP model using the ANN algorithm, it has been coded within the Python 3.11 environment and executed on the database. The number of neurons in the input and output layers is configured to align with the quantity of input parameters (AF,

FR, and GSI) and output parameter (ROP), respectively. Meanwhile, the number of neurons in the hidden layers is adjusted based on the complexity of the problem. Consequently, finding the optimal number of neurons becomes essential.

**Figure 14** shows the sensitivity analysis on the number of neurons. According to the figure, sensitivity analysis was conducted by varying the number of neurons from 3 to 300 in the hidden layers. In the end, the optimal number of neurons selected for achieving the highest accuracy is 100 neurons. **Figure 15** shows the relationship between the predicted and measured values of the ANN model, utilizing 100 neurons.

**Performance evaluation of developed models**

In order to assess the performance of the developed models, three evaluation metrics have been employed: Normalized Root Mean Square Error (NRMSE), Variance Accounted For (VAF), and Coefficient of Determination (R2). These metrics will be computed using the formulas provided in Eqs. (4) to (6) [57,58] using Monte Carlo simulation, the penetration rate is predicted, and the sensitivity of the parameters affecting the penetration rate in the TBM machine is evaluated. For this purpose, a database containing in-situ rock properties, rock mass characteristics, and mechanical parameters related to TBM in the Queens Water transfer tunnel has been used. A mathematical model has been developed using principal component analysis to simulate. The results of evaluating the performance of the developed model showed that the model has acceptable performance (VAF = 84.4%, RMSE = 0.03, NSE = 0.82, and R2 = 0.84).

$$NRMSE = \frac{\sqrt{\frac{1}{N} \sum_{i=1}^N (A_i - P_i)^2}}{A_{avg}} \quad (4)$$

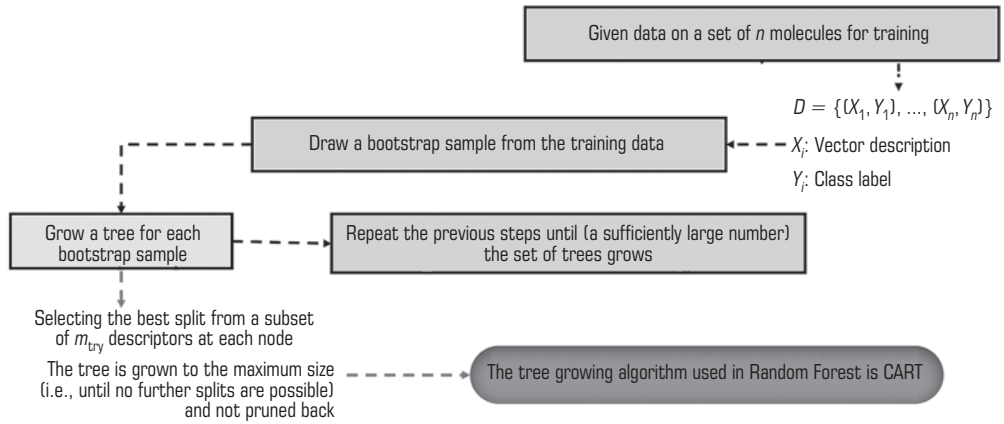


**Fig. 11. The training procedure of the RF algorithm**

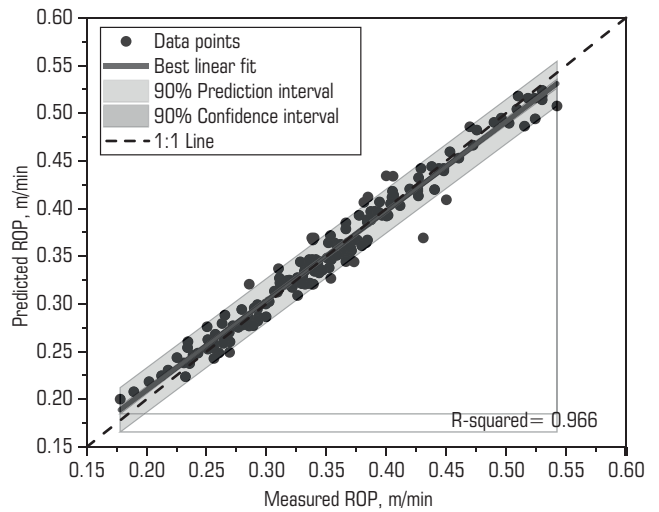


**Fig. 12. The relationship between predicted and measured values of RF model**

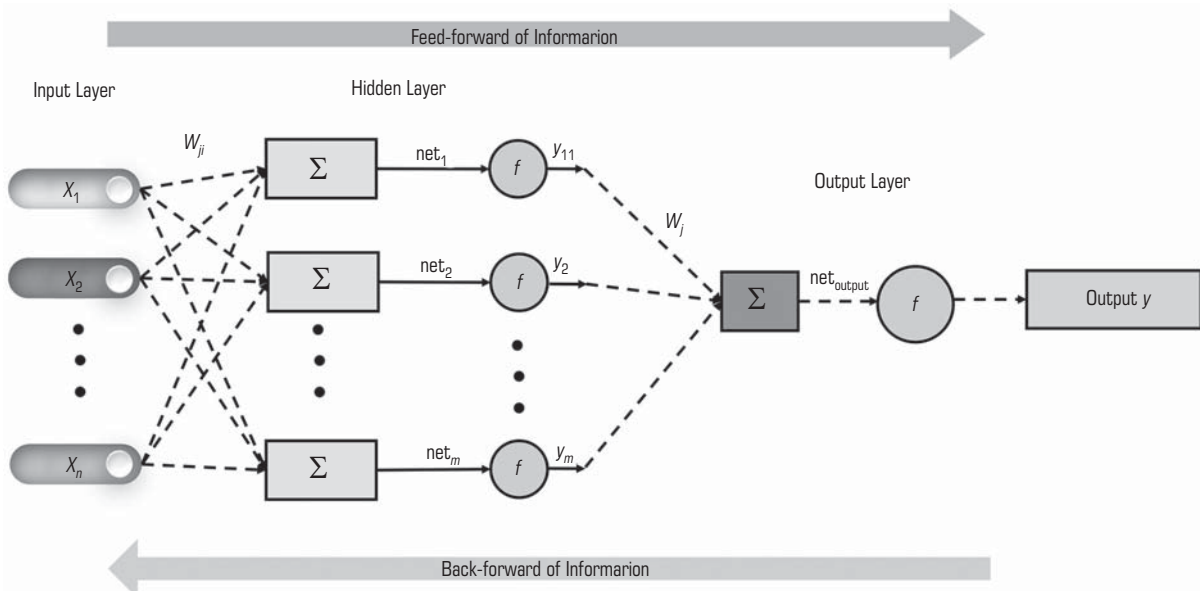


**Fig. 13. The schematic representation of the implemented MLP algorithm**

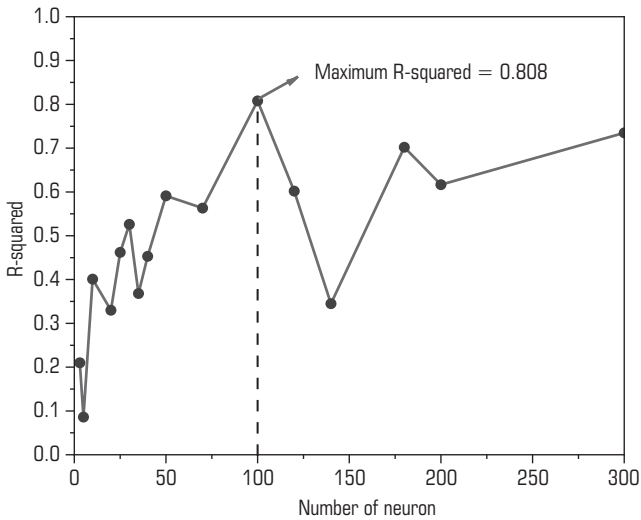


Fig. 14. The sensitivity analysis on the number of neurons

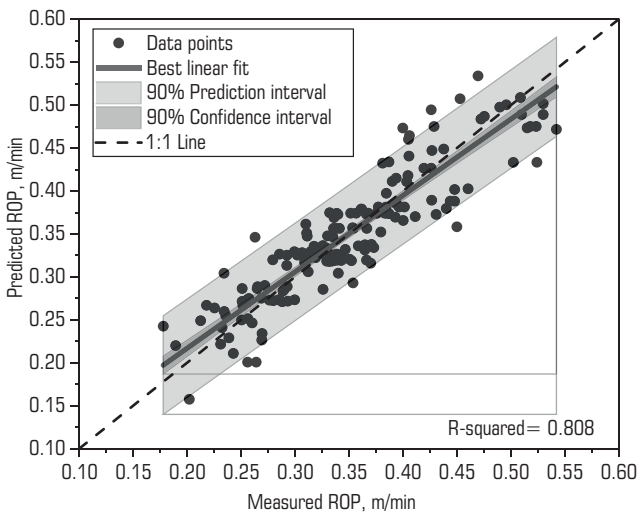


Fig. 15. The relationship between predicted and measured values of ANN model

$$VAF = \left[ 1 - \frac{\text{var}(A_i - P_i)}{\text{var}(A_i)} \right] \times 100, \quad (5)$$

$$R2 = \frac{\left( \sum_{i=1}^N (P_i - \bar{P})(A_i - \bar{A}) \right)^2}{\sqrt{\sum_{i=1}^N (P_i - \bar{P})^2 \sum_{i=1}^N (A_i - \bar{A})^2}}, \quad (6)$$

where  $P_i$  is the predicted values;  $A_i$  is the measured values;  $\bar{P}$  is the average of the  $P_i$ ;  $N$  is the number of data;  $\bar{A}$  is the average of the  $R_i$ .

Theoretically, a predictive correlation is considered excellent when the  $R2$  equals 1, the  $NRMSE$  approaches 0, and the  $VAF$  reaches 100%. Figure 16 shows the performance evaluation of the developed SVM, ANN, and RF models. Based on the obtained results, the RF model demonstrates superior performance in ROP evaluation compared to the ANN and SVM models. The RF model achieves both high accuracy and low uncertainty. However, a limitation of all three SVM, ANN, and RF models is their status as black boxes, which implies that they cannot offer an explicit equation for ROP evaluation. Instead, the output can be derived through the Python code implementation.

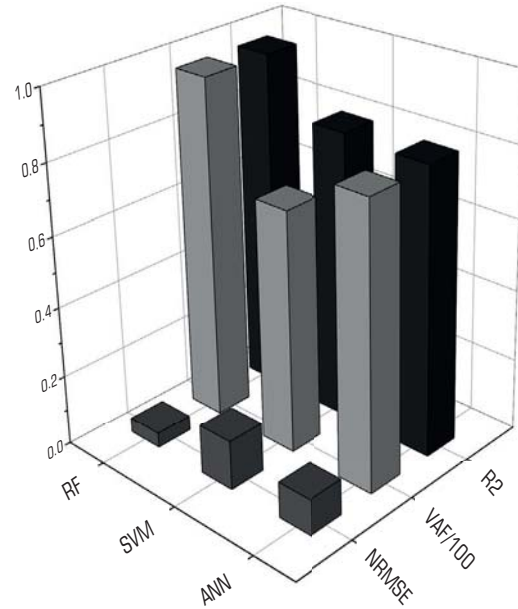


Fig. 16. The performance evaluation of the developed models

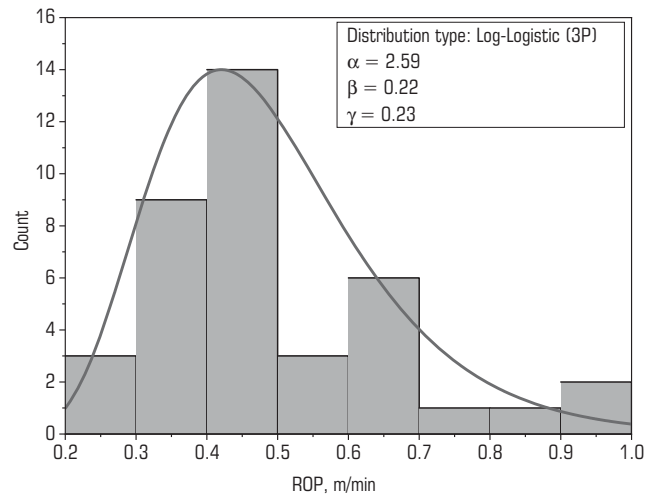
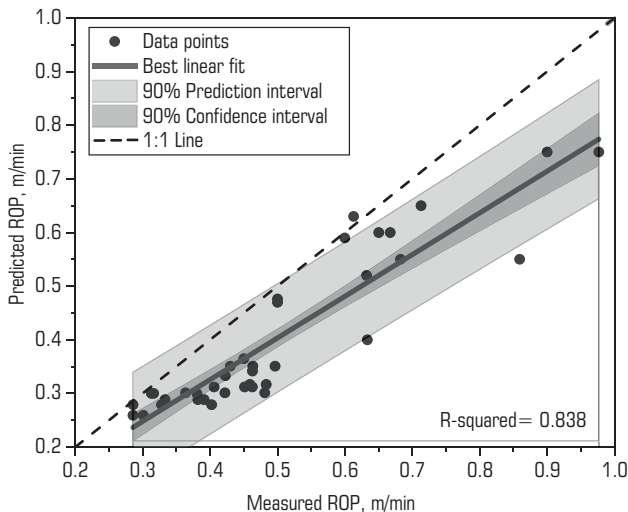


Fig. 17. The ROP distribution of the Anarak copper mine

### Application of developed model

In this section, developed models are used to evaluate the ROP of Anarak copper mine. According to the developed models, the RF model showed the best performance compared to the SVM and ANN models. Consequently, the RF model is employed for evaluating the ROP of the Anarak copper mine. It should be noted that the drilling operation in all four mining zones (waste, low grade, moderate grade, and high grade) was conducted using two parameters, AF and FR. To minimize errors, each parameter was repeated nine times, and ultimately, the average results were taken into consideration as the final output. Figure 17 shows the ROP distribution of the Anarak copper mine. According to the figure, the distribution of the mine's ROP follows a log-logistic (3P) pattern. Finally, the ROP results obtained from the RF model are compared with those obtained from drilling operations. To utilize the RF model for predicting ROP, it was coded within the Python environment to perform automatic evaluations on the data obtained during the drilling of the Anarak mine. Figure 18 displays the results of the ROP evaluation for the Anarak copper mine. According to the obtained results, the RF model has been able to predict the ROP in Anarak copper mine with 83.8% accuracy.





**Fig. 18. The results of the ROP evaluation for the Anarak copper mine based on RF model**

### Summary and conclusions

The use of rock drilling has been prevalent in a variety of construction, mining, and oil projects over the years. The timing of the drilling operation as the initial step in the mining activity has an impact on the productivity of the mine. Hence, the drilling ROP is regarded as a crucial parameter for production planning, and it is imperative to assess and maximize the ROP based on the optimal conditions of drilling operations in each project. In this study, the first step involved applying Taguchi's algorithm to two parameters influencing the ROP: feed rate pressure and air flushing pressure. The objective was to create an experimental design aimed at maximizing the ROP. Subsequently, the developed design was tested during mining operations at the Anarak copper mine in Isfahan, Iran. This mine was divided into four zones based on copper grade and GSI value, and drilling operations were carried out for each of the zones using ROC-D65 drill wagons. Finally, optimal drilling operating conditions were recommended for each zone, with the aim of achieving the highest ROP. Subsequently, a database comprising 170 cases of hole drilling with a drill wagon in the Sarchesme copper mine in Kerman, Iran, was compiled. Using the Python environment, two models were constructed, employing SVM, ANN, and RF algorithms, to predict the ROP. The results indicate that when the copper grade rises and rock strength decreases (in the crushed zone), the air flushing pressure exhibits the most significant impact on the drilling ROP. Conversely, when the copper grade decreases and rock strength increases, the feed rate pressure becomes the predominant factor affecting the drilling ROP. Additionally, as both air flushing pressure and feed rate pressure increase, the drilling ROP also increases. Nevertheless, an excessive rise in feed rate pressure can result in a decrease in the ROP, eventually leading to the drilling bit getting stuck. The results of the performance of the developed models showed that among the algorithms used (accuracy ranging from 80.8% to 96.6%), the RF model demonstrated better performance than SVM and ANN in predicting drilling ROP (VAF = 96.564, NRMSE = 0.042, and R<sup>2</sup> = 0.966). Based on the performance obtained, the developed RF model was utilized to evaluate the ROP at the Anarak copper mine. Since the model lacks explicit mathematical equations and functions as a black box, it was implemented in the drilling operation using Python coding. After drilling operations in each zone, the actual ROP was compared with the predicted value. The results demonstrated that the developed model can accurately predict the ROP with an accuracy of 83.8%. Therefore, based on validation, the RF model serves as a reliable predictor for ROP in drilling projects with low uncertainty. Project managers can employ it to estimate initial scheduling and associated costs for drilling projects during early tender stages or throughout mining operations.

### References

1. Rafezi H, Hassani F. Drilling signals analysis for tricone bit condition monitoring. *International Journal of Mining Science and Technology*. 2021. Vol. 31, Iss. 2. pp. 187–195.
2. Vogt D. A review of rock cutting for underground mining: past, present, and future. *Journal of the Southern African Institute of Mining and Metallurgy*. 2016. Vol. 116. pp. 1011–1026.
3. Wang J., Gu D., Yu Z., Tan C., Zhou L. A framework for 3D model reconstruction in reverse engineering. *Computers & Industrial Engineering*. 2012. Vol. 63, Iss. 4. 1189–1200.
4. Bilgin A., Yalcin E., Kutbay H., Kilinc M. Nutrient Concentrations and Biomass in Lake Vegetation and Nutrient Limitation in Lakes of Northern Black Sea Region of Turkey. *Ekologia (Bratislava)*. 2003. Vol. 22, Iss. 3. pp. 257–268.
5. Moein M. J. A, Shaabani E., Rezaeian M. Experimental evaluation of hardness models by drillability tests for carbonate rocks. *Journal of Petroleum Science and Engineering*. 2014. Vol. 113. pp. 104–108.
6. Paone J. Drillability studies: impregnated diamond bits. Michigan : University of Michigan Library. 1966. Vol. 6776. 24 p.
7. Howarth D. F., Adamson W. R., Berndt J. R. Correlation of model tunnel boring and drilling machine performances with rock properties. *International Journal of Rock Mechanics and Mining Sciences & Geomechanics Abstracts*. 1986. Vol. 23. pp. 171–175.
8. Thakur M., Choudhary B. S., Seervi V. An Investigation into the Effect of Rock Properties on Drill Bit Life. *Journal of The Institution of Engineers (India): Series D*. 2023. DOI: 10.1007/S40033-023-00542-2
9. Hoseinie S. H, Ghorbani S., Ghodrati B. Selection of suitable drilling method in Razgha nepheline syenite mine, a systematic approach. *Eurasian Mining*. 2020. No. 1. pp. 56–60.
10. Shigin A. O, Gilyov A. V., Shigina A. A. Automation of rotary blasthole drilling in open pit mines. *Gornyi Zhurnal*. 2017. No. 2. pp. 82–86.
11. Kahraman S. Correlation of TBM and drilling machine performances with rock brittleness. *Engineering Geology*. 2002. Vol. 65, Iss. 4. pp. 269–283.
12. Rajesh Kumar B., Vardhan H., Govindaraj M., Vijay G. S. Regression analysis and ANN models to predict rock properties from sound levels produced during drilling. *International Journal of Rock Mechanics and Mining Sciences*. 2013. Vol. 58. pp. 61–72.
13. Kumar B. R, Vardhan H., Govindaraj M. Sound level produced during rock drilling vis-à-vis rock properties. *Engineering Geology*. 2011. Vol. 123, Iss. 4. pp. 333–337.
14. Bezminabadi S. N, Ramezanzadeh A., Esmail Jalali S. M, Tokhmechi B., Roustaei A. Effect of rock properties on ROP modeling using statistical and intelligent methods: A case study of an oil well in southwest of Iran. *Archives of Mining Sciences*. 2017. Vol. 62: pp. 131–144.
15. Kahraman S., Bilgin N., Feridunoglu C. Dominant rock properties affecting the penetration rate of percussive drills. *International Journal of Rock Mechanics and Mining Sciences*. 2003. Vol. 40, Iss. 5. pp. 711–723.
16. Abu Bakar M. Z., Butt I. A., Majeed Y. Penetration Rate and Specific Energy Prediction of Rotary–Percussive Drills Using Drill Cuttings and Engineering Properties of Selected Rock Units. *Journal of Mining Science*. 2018. Vol. 54. pp. 270–284.
17. Basarir H., Tutluoglu L., Karpuz C. Penetration rate prediction for diamond bit drilling by adaptive neuro-fuzzy inference system and multiple regressions. *Engineering Geology*. 2014. Vol. 173. pp. 1–9.
18. Delavar M. R, Ramezanzadeh A., Tokhmechi B. An investigation into the effect of geomechanical properties of reservoir rock on drilling parameters — a case study. *Arabian Journal of Geosciences*. 2021. Vol. 14. pp. 1–25.
19. Karpuz C., Pasamehmetoglu A. G., Dincer T., Muftuoglu Y. Drillability studies on the rotary blasthole drilling of lignite overburden series. *International Journal of Mining Reclamation and Environment*. 1990. Vol. 4. pp. 89–93.
20. Paone J. Drillability studies: statistical regression analysis of diamond drilling. Michigan : University of Michigan Library, 1966. 40. p.

21. Akün M. E., Karpuz C. Drillability studies of surface-set diamond drilling in Zonguldak region sandstones from Turkey. *International Journal of Rock Mechanics and Mining Sciences*. 2005. Vol. 42, Iss. 3, pp. 473–479.
22. Ersoy A., Waller M. Prediction of drill-bit performance using multivariable linear regression analysis. *International Journal of Rock Mechanics and Mining Sciences and Geomechanics Abstracts*. 1995. Vol. 6.
23. Yinchol H., Kumdol P., Jianming P. et al. Analysis of effects of operating parameters on rate of penetration in drilling process with air down-the-hole hammer. *Global Geology*. 2021. Vol. 24. pp. 64–70.
24. Eren T., Ozbayoglu M. E. Real Time Optimization of Drilling Parameters During Drilling Operations. *SPE Oil and Gas India Conference and Exhibition*. 2010. DOI: 10.2118/129126-MS
25. Soares C., Gray K. Real-time predictive capabilities of analytical and machine learning rate of penetration (ROP) models. *Journal of Petroleum Science and Engineering*. 2019. Vol. 172. 934–959.
26. Riazi M., Mehrjoo H., Nakhaei R. et al. Modelling rate of penetration in drilling operations using RBF, MLP, LSSVM, and DT models. *Scientific Reports*. 2022. Vol. 12. ID 11650.
27. Bourgoyne A. T., Young F. S. A Multiple Regression Approach to Optimal Drilling and Abnormal Pressure Detection. *Society of Petroleum Engineers Journal*. 1974. Vol. 14, Iss. 4. pp. 371–384.
28. Hegde C., Daigle H., Millwater H., Gray K. Analysis of rate of penetration (ROP) prediction in drilling using physics-based and data-driven models. *Journal of Petroleum Science and Engineering*. 2017. Vol. 159. pp. 295–306.
29. Hustrulid W. A., Fairhurst C. A theoretical and experimental study of the percussive drilling of rock part III—experimental verification of the mathematical theory. *International Journal of Rock Mechanics and Mining Sciences & Geomechanics Abstracts*. 1972. Vol. 9, Iss. 3. pp. 417–429.
30. Kahraman S. Rotary and percussive drilling prediction using regression analysis. *International Journal of Rock Mechanics and Mining Sciences*. 1999. Vol. 36. pp. 981–989.
31. Karna S., Sahai R. An overview on Taguchi method. *International Journal of Engineering and Mathematical Sciences*. 2012. Vol. 1. pp. 1–7.
32. Vellaiyan S., Amirthagadeswaran K., Sivasamy D. Taguchi-Grey Relation Based Multi-response Optimization of Diesel Engine Operating Parameters with Water-in Diesel Emulsion Fuel. *International Journal of Technology*. 2018. Vol. 9, No. 1. 68–77.
33. Sumesh A., Shibu M. Optimization of drilling parameters for minimum surface roughness using Taguchi method. *IOSR Journal of Mechanical and Civil Engineering (IOSR-JMCE)*. 2016. pp. 12–20.
34. Kumar R., Chohan J. S., Singh S. et al. Implementation of Taguchi and Genetic Algorithm Techniques for Prediction of Optimal Part Dimensions for Polymeric Biocomposites in Fused Deposition Modeling. *International Journal of Biomaterials*. 2022. DOI: 10.1155/2022/4541450.
35. Pradhan B., Jebur M. N., Shafri H. Z. M., Tehrani M. S. Data fusion technique using wavelet transform and taguchi methods for automatic landslide detection from airborne laser scanning data and quickbird satellite imagery. *IEEE Transactions on Geoscience and Remote Sensing*. 2016. Vol. 54, Iss. 3. pp. 1610–1622.
36. Molaei N., Razavi H., Chehreh Chelgani S. Designing different beneficiation techniques by Taguchi method for upgrading Mehdi-Abad white barite ore. *Mineral Processing and Extractive Metallurgy Review*. 2018. Vol. 39, Iss. 3. pp. 198–201.
37. Baradeswaran A., Elayaperumal A., Franklin Issac R. A Statistical Analysis of Optimization of Wear Behaviour of Al-Al<sub>2</sub>O<sub>3</sub> Composites Using Taguchi Technique. *Procedia Engineering*. 2013. Vol. 64. pp. 973–982.
38. Suhane A., Sarviya R. M., Siddiqui A. R., Khaira H. K. Optimization of Wear Performance of Castor Oil based Lubricant using Taguchi Technique. *Materials Today: Proceedings*. 2017. Vol. 4. pp. 2095–2104.
39. Kang H., Park J. Y., Cho J. W. et al. Optimal button arrangement of a percussion drill bit and its operating condition for improving drilling efficiency. *Journal of Mechanical Engineering Science*. 2017. Vol. 232, Iss. 16. pp. 2887–2898.
40. Karpov V. N., Petreev A. M. Determination of Efficient Rotary Percussive Drilling Techniques for Strong Rocks. *Journal of Mining Science*. 2021. Vol. 57. pp. 447–458.
41. Hoek E., Brown E. T. The Hoek–Brown failure criterion and GSI – 2018 edition. *Journal of Rock Mechanics and Geotechnical Engineering*. 2019. Vol. 11, Iss. 16. pp. 445–463.
42. Hussian S., Mohammad N., Ur Rehman Z. et al. Review of the geological strength index (GSI) as an empirical classification and rock mass property estimation tool: Origination, modifications, applications, and limitations. *Advances in Civil Engineering*. 2020. DOI: 10.1155/2020/6471837
43. Aboutaleb S., Behnia M., Bagherpour R., Bluekian B. Using non-destructive tests for estimating uniaxial compressive strength and static Young's modulus of carbonate rocks via some modeling techniques. *Bulletin of Engineering Geology and the Environment*. 2018. Vol. 77. pp. 1717–1728.
44. Cristianini N., Shawe-Taylor J. An introduction to support vector machines and other kernel-based learning methods. Cambridge : Cambridge University Press, 2000. 189 p.
45. Breiman L. Random forests. *Machine Learning*. 2001. Vol. 45. pp. 5–32.
46. Biau G. Analysis of a random forests model. *The Journal of Machine Learning Research*. 2012. Vol. 13. pp. 1063–1095.
47. Kohestani V. R., Bazarganlari M. R., Asgari Marnani J. Prediction of maximum surface settlement caused by earth pressure balance shield tunneling using random forest. *Journal of AI and Data Mining*. 2017. Vol. 5. pp. 127–135.
48. Tao H., Wang J., Zhang L. Prediction of hard rock TBM penetration rate using random forests. *The 27th Chinese Control and Decision Conference (2015 CCDC)*. 2015. pp. 3716–3720. DOI: 10.1109/CCDC.2015.7162572
49. Svetnik V., Liaw A., Tong C. et al. Random forest: a classification and regression tool for compound classification and QSAR modeling. *Journal of Chemical Information and Computer Sciences*. 2003. Vol. 43, No. 6. pp. 1947–1958.
50. McCulloch W. S., Pitts W. A logical calculus of the ideas immanent in nervous activity. *The Bulletin of Mathematical Biophysics*. 1943. Vol. 5. pp. 115–133.
51. Ghasemi E., Amini H., Ataei M., Khalokakaei R. Application of artificial intelligence techniques for predicting the flyrock distance caused by blasting operation. *Arabian Journal of Geosciences*. 2014. Vol. 7. pp. 193–202.
52. Engelbrecht A. Computational intelligence: an introduction. England : John Wiley & Sons, 2007. 597 p.
53. Saghatforoush A., Monjezi M., Faradonbeh S. R., Armaghani J. D. Combination of neural network and ant colony optimization algorithms for prediction and optimization of flyrock and back-break induced by blasting. *Engineering with Computers*. 2016. Vol. 32. pp. 255–266.
54. Momeni E., Armaghani J. D., Hajihassani M., Mohd Amin M. F. Prediction of uniaxial compressive strength of rock samples using hybrid particle swarm optimization-based artificial neural networks. *Measurement*. 2015. Vol. 60. pp. 50–63.
55. Monjezi M., Mehrdaneh A., Malek A., Khandelwal M. Evaluation of effect of blast design parameters on flyrock using artificial neural networks. *Neural Computing and Applications*. 2013. Vol. 23. pp. 349–356.
56. Lee D. H., Kim Y. T., Lee S. R. Shallow Landslide Susceptibility Models Based on Artificial Neural Networks Considering the Factor Selection Method and Various Non-Linear Activation Functions. *Remote Sensing*. 2020. Vol. 12, Iss. 7. ID 1194.
57. Jafarshirzad P., Ghasemi E., Yagiz S., Kadkhodaei M. H. Evaluation of Hard Rock Tunnel Boring Machine (TBM) Performance Using Stochastic Modeling. *Geotechnical and Geological Engineering*. 2023. Vol. 41. pp. 3513–3529.
58. Ghorbani S., Hoseinie S. H., Ghasemi E., Sherzadeh T. Effect of quantitative textural specifications on Vickers hardness of limestones. *Bulletin of Engineering Geology and the Environment*. 2023. Vol. 82, No. 32. DOI: 10.1007/S10064-022-03049-4 **EM**